Colloid Polym Sci (2006) 284: 387–395
DOI 10.1007/s00396-005-1395-1

ORIGINAL CONTRIBUTION

V. V. A. Fernandez
N. Tepale
J. C. Sánchez-Díaz
E. Mendizábal
J. E. Puig
J. F. A. Soltero

Thermoresponsive nanostructured poly (*N*-isopropylacrylamide) hydrogels made via inverse microemulsion polymerization

Received: 19 April 2005
Revised: 15 August 2005
Accepted: 22 August 2005
Published online: 23 September 2005

V. V. A. Fernandez · N. Tepale
J. E. Puig · J. F. A. Soltero (✉)
Departamento de Ingeniería Química,
Universidad de Guadalajara,
Boul. M. García Barragán# 1451,
Guadalajara 44430, Mexico
E-mail: armandosolteros@yahoo.com
Tel.: +52-33-36503401
Fax: +52-33-36503401

J. C. Sánchez-Díaz · E. Mendizábal
Departamento de Química,
Universidad de Guadalajara,
Boul. M. García Barragán# 1451,
Guadalajara 44430, Mexico

Abstract The synthesis of nanostructured poly(*N*-isopropylacrylamide) (polyNIPA) hydrogels by a two-stage polymerization process is reported here. The process involves the synthesis of slightly crosslinked polyNIPA nanoparticles by inverse (w/o) microemulsion polymerization; then, these particles are dried, cleaned and dispersed in an aqueous solution of NIPA and a crosslinking agent (*N*,*N*-methylene-bis-acrylamide or NMBA) and polymerized to produce the nanostructured hydrogels. Their swelling and de-swelling kinetics, volume phase transition temperatures (T_{VPT}) and mechanical properties at the equilibrium swollen state are investigated as a function of the weight ratio of polyNIPA particles to monomer (NIPA). The nanostructured gels exhibit larger equilibrium water uptake, faster swelling and de-swelling rates and similar T_{VPT} than those of the conventional ones; moreover, the elastic and Young moduli are larger than those of the conventional hydrogels at similar swelling ratios. The fast swelling and de-swelling kinetics are explained in terms of the controlled inhomogeneities introduced by the method of synthesis.

Keywords Poly(*N*-isopropylacrylamide) · PolyNIPA hydrogel Microemulsion · Nanostructured hydrogel · Thermoresponsive hydrogel

Introduction

Poly(*N*-isopropylacrylamide) (polyNIPA) is a thermoresponsive polymer that has a lower critical solution temperature (LCST) of 32 °C in water [1]. Below the LCST, polyNIPA and water are completely miscible; above the LCST, phase separation occurs. As a consequence of this transition, crosslinked polyNIPA hydrogels exhibit a volume phase transition at around 34 °C [2]. It has been proposed that this transition takes place because the hydrogen bonding interactions that form stable hydration shells around the hydrophobic groups of polyNIPA disappear and that the hydrophobic interactions among polymer chains increase above the LCST, which cause expulsion of water [2, 3]. However, recent ^{1}H-NMR studies on polyNIPA hydrogels reveal that the diffusion coefficient of water diminishes and that the amount of bound water increases as the volume phase transition temperature is approached [4, 5], contrary to previous proposals [2]. Below the volume phase transition temperature, the gel is highly hydrated; above this temperature, it is in a collapsed state due to the expulsion of water. Inasmuch as this transition is reversible, polyNIPA and other thermoresponsive hydrogels are especially useful for on–off switches for modulated drug delivery systems [6–13], tissue engineering and artificial organs [13–16], in separation processes [17, 18], in protein–ligand recognition [19], as thermoresponsive gates [20] and in enzyme and cell immobilization [21, 22].

For many applications, hydrogels with large water absorption capacity and favorable mechanical proper-

ties in the swollen state are required [23–25]. Usually, an increase in the swelling is accompanied with a decrease in the mechanical properties [23, 24, 26, 27]. These properties as well as others, such as transparency and oxygen permeability, can be usually modified by: (1) changing the hydrophilic monomer, (2) modifying the concentration and type of the crosslinking agent, (3) varying the method of preparation, or (4) by copolymerizing hydrophilic and hydrophobic monomers [28–30]. The synthesis of hydrogels is typically accomplished by free radical polymerization (although step polymerization has also been used) or by modification or functionalization of existing polymers [30]. In the first type, mass or solution polymerization is commonly employed, although suspension, emulsion and microemulsion polymerization processes—to produce nano- and microgels—have also been used [31, 32].

For thermoresponsive hydrogels, the rapid response to temperature changes is the most essential function for many important applications. In this respect, efforts to increase the response kinetics have been forwarded. Some authors have improved the shrinking kinetics by making a heterogeneous polyNIPA network structure by phase separation methods [33, 34]. Others have synthesized fast swelling and de-swelling polyNIPA hydrogels by introducing free-end (graft) chains [35–37]. Zhang and Zhuo improved the response rate by incorporating siloxane linkages, cold polymerization and crosslinking methods [38–41]. These authors also obtained rapid shrinking polyNIPA materials by cold treatment followed by thawing [42]. Zhang et al. synthesized rapid-response and highly swollen polyNIPA hydrogels with macroporous network structure by incorporating poly(ethylene glycol) (PEG) of different molecular weights; since the PEG did not participate in the reaction, this polymer only acts as a pore-forming agent during the polymerization [43]. Shibayama's group has studied the effect of NIPA and crosslinking agent (NMBA) as well as the preparation and destination temperatures on the de-swelling kinetics of polyNIPA hydrogels [44–48].

Recently, we reported the synthesis by a two-stage polymerization process of nanostructured polyacrylamide gels that swell faster and have larger equilibrium water uptakes than the conventional hydrogels with similar composition and degree of crosslinking [27]. Moreover, the nanostructured materials have larger Young modulus at similar or even larger degrees of swelling than conventional hydrogels [27]. Highly swollen nanostructured hydrogels based on star-polymers can also be synthesized by living polymerization techniques. Keys et al. [49] made PEG start-hydrogels by γ-irradiation; these hydrogels exhibited high water absorption ratios but were fragile. These authors increased the swelling ratio by the incorporation of acrylate groups and copolymerization with poly(ethylene glycol) diacrylate. Lutz [50] made star-shaped poly(ethylene oxide)-based hydrogels by free radical polymerization in heterogeneous medium using multifunctional anionic initiators; these hydrogels, being biocompatible, have found applications as permeable membranes for artificial pancreas and as templates for the growth of nervous cell. Vamvakaki et al. [51] synthesized crosslinked start-hydrogels by group transfer polymerization, using 2-(dimethylamino)ethyl methacrylate as monomer and ethylene gycol as the crosslinking agent; the swelling of these hydrogels were pH-sensitive. However, in none of these papers, the mechanical properties of these highly swollen start-polymer hydrogels were reported.

Here, we report the synthesis of nanostructured polyNIPA hydrogels by a similar two-stage polymerization method. These hydrogels have larger swelling, faster swelling and de-swelling rates and better mechanical properties than the conventional hydrogels with similar overall polymer concentration and crosslinking degree. Moreover, the volume phase transition temperature (T_{VPT}) of these nanostructured hydrogels is similar to that of the conventional polyNIPA hydrogels (ca. 34 °C).

Experimental

Sodium bis(2-ethylhexyl)sulfosuccinate (Aerosol OT or AOT), 98% pure from Fluka, was dried and stored in a desiccator jar prior to use. *N*-isopropylacrylamide (NIPA), 99% pure from TCI Tokyo Kasei, was used without further purification. *N*, *N*-methylenebisacrylamide (NMBA) from Scientific Polymer Products was recrystallized from methanol. Benzoyl peroxide (BP), 99% pure, and potassium persulfate (KPS), 97% pure, both from Aldrich, were used without further purification. *N*,*N*,*N*,*N*-tetramethylethylenediamine (TMEDA) from TCI Tokyo Kasei was used without further purification. Doubly distilled and deionized water was drawn from a Millipore purification system. Toluene was 99% pure from Lancaster Synthesis. Methanol was 99.9% pure from Fermont.

Thermoresponsive nanostructured hydrogels were made by a two-stage polymerization process. First NIPA was polymerized at 25 °C in inverse (w/o) microemulsions using BP ($m_{BP}/m_{NIPA} = 0.01$) and TMEDA ($m_{TMEDA}/m_{NIPA} = 0.03$) as the redox-pair initiation system. The parent w/o microemulsion composition was 65.7 wt.% toluene, 14.7 wt.% AOT and 15.68 wt.% H_2O and 3.92 wt.% NIPA ($m_{NIPA}/m_{H_2O} = 0.25$). To preserve the shape and size of the particles during handling and in the second polymerization stage, the crosslinking agent NMBA ($m_{NMBA}/m_{NIPA} = 0.01$) was also added to the microemulsion before polymerization. The polymerization yields bluish inverse latex containing the polyNIPA nanoparticles. To isolate the particles,

most of the toluene and water were removed from the latex by distillation at 107 °C; the resulting viscous solution was dried in an oven at 50 °C for 24 h. To remove the adsorbed AOT from the particles, excess methanol, which is a good solvent for AOT, was added to the dried residue and filtered. For the second polymerization stage, the particles were dried in an oven at 50 °C for 24 h and then dispersed in an aqueous solution of NIPA and NMBA ($m_{NMBA}/m_{NIPA} = 0.01$) and polymerized in test tubes for 2 h at 25 °C with KPS as initiator ($m_{KPS}/m_{NIPA} = 0.01$) and TMEDA as accelerator ($m_{TMEDA}/m_{NIPA} = 0.01$). In the second stage regardless of the weight ratio of particles to NIPA ($m_{particles}/m_{NIPA}$), which was varied from 0/100 to 30/70, the ratio of (monomer + particles) to water weight was 1/10. Conventional hydrogels were made by polymerization of aqueous solution of NIPA (0.1 g of NIPA/ml of water) and varying concentrations of NMBA ($0.001 \le w_{NMBA}/w_{NIPA} \le 0.01$) for 2 h at 25 °C with KPS ($m_{KPS}/m_{NIPA} = 0.01$) and TMEDA ($m_{TMEDA}/m_{NIPA} = 0.01$) in test tubes.

The size of the particles obtained by inverse microemulsion polymerization was measured with a Malvern 4700C quasielastic light-scattering (QLS) apparatus. Intensity correlation data were analyzed by the method of cumulants to provide the average decay rate, $\langle \Gamma \rangle$ ($= q^2 D$), where q is the magnitude of the scattering vector and D is the diffusion coefficient. The measured diffusion coefficients were represented in terms of apparent diameters by means of Stokes law assuming that the solvent has the viscosity of toluene. Inverses lattices were measured without dilution.

The hydrogels, in the shape of cylinders, were cut to yield disks of 1 cm in thickness. These disks were immersed in doubly distilled and deionized water for a week to remove residual monomer and surfactant, and dried in an oven at 40 °C to constant weight. The dried disks (xerogels) were sanded with mild sandpaper until their diameters and thicknesses were ca. 8 and 2 mm, respectively. Then the sanded disks were weighed and immersed in water and their swelling kinetics were followed at constant temperature by removing the hydrogels from the water at given times, blotting them with a paper towel and weighing. The water uptake of the hydrogels, H_p, was calculated as:

$$H_p = \left(\frac{m(t) - m_0}{m_0} \right). \tag{1}$$

Here $m(t)$ and m_0 represent the weights of the hydrogel at time t and of the xerogel, respectively.

To study the effect of temperature on the equilibrium water uptake ($H_{p\infty}$), the procedure was the following. The sample was immersed in a constant-temperature bath until $H_{p\infty}$ was reached. $H_{p\infty}$ was determined by removal and weighing of the hydrogel as described above, until its weight did not change after several measurements taken in a span of an hour; this weight was used to calculate $H_{p\infty}$ with Eq. 1. Then the temperature of the water bath was increased and the procedure was repeated.

For de-swelling kinetics measurements, the hydrogels at equilibrium water uptake at 25 °C were cut with a punch, to ensure that the dimensions of the disks at equilibrium swelling were similar. Then the disks were immersed again in water at 25 °C and the diameter of each disk was measured using a previously calibrated video camera. Then, the disks were immersed in water at 40 °C and the de-swelling was followed by measuring their diameters as a function of time with the video camera. To estimate the degree of de-swelling at each time, it was assumed that the sample de-swells isotropically.

The de-swelling data were fitted with a modified Flory–Rehner equation given by [46]:

$$\begin{aligned} & v \frac{C_{NIPA}}{C_{NIPA,0}} \left[\frac{1}{2} \left(\frac{\phi}{\phi_0} \right) - \left(\frac{\phi}{\phi_0} \right)^{\frac{1}{3}} \right] \\ & - \frac{1}{V_s} \left[\phi + \ln(1-\phi) + \left[\frac{(\Delta H - T\Delta S)}{k_B T} + \phi \chi_2 \right] \phi^2 \right] \\ & = 0 \end{aligned} \tag{2}$$

In this equation, $C_{NIPA,0}$ is the reference NIPA concentration, which is a lower bound of NIPA concentration capable of gel formation (ca. 300 mM [45]); V_s is the molar volume of the solvent, χ_2 is the Flory's interaction parameter; ΔH and ΔS are the changes in enthalpy and entropy per monomer unit of network related to the volume transition; k_B is the Boltzmann constant; T is the temperature; ϕ and ϕ_0 are the network volume fraction at swelling equilibrium and the reference state, respectively; ϕ_0 is obtained from [44]:

$$\phi_0 \approx \frac{V_{NIPA}}{1,000} C_0. \tag{3}$$

In this equation, C_0 is the NIPA monomer concentration used in the second polymerization stage.

The swelling ratio ϕ / ϕ_0 is related to d/d_0 as follows:

$$\frac{\phi_0}{\phi} = \left(\frac{d}{d_0} \right)^3. \tag{4}$$

The number density of crosslinks ν can be estimated as follows:

$$v = \frac{2C_{NMBA}}{C_{NIPA}} \frac{\phi_0}{V_{NIPA}} = \frac{2C_{NMBA}}{1,000}. \tag{5}$$

Here, C_{NMBA} is the NMBA concentration.

The volume phase transition temperature was determined as a function of the weight ratio of polyNIPA

particles to monomer ($m_{particles}/m_{NIPA}$) with a T/A Instruments Q100 differential scanning calorimeter (DSC) apparatus at a heating rate of 5 °C. Here, the T_{VPT} is taken as the temperature where the heat flow takes a minimum.

Hydrogels at their equilibrium water uptakes with $m_{particles}/m_{NIPA}$ of 0/100 and 30/70 were freeze-dried and fractured in liquid nitrogen to examine their microstructures in a JEOL 5400 LV scanning electron microscope (SEM). An electron beam with accelerating voltage of 20 kV was used on each sample. Samples corresponding to the outer and inner surfaces were placed in brass holders and coated with a thin gold film to enhance image resolution using an EMS-76 coating machine (Ernest F. Fullam) with an applied current of 60 mA for 2 min.

The mechanical properties were measured at 25 °C in a Perkin-Elmer TMA-7 thermo-mechanical analyzer instrument with a compression probe. Hydrogel disks of known dimensions at equilibrium water uptake were immersed in a homemade chamber full of water with the aim to maintain dynamic equilibrium swelling during measurements. The elastic (G) and Young (E) moduli were estimated in the linear deformation region according to [52]:

$$\tau = E(\lambda - 1) \tag{6}$$

and

$$\tau = G(\lambda - \lambda^{-2}). \tag{7}$$

Here τ is the compressing stress and λ ($= l/l_0$) is the deformation strain, l_o and l being the original and deformed thicknesses, respectively.

Results

The z-average diameter of the particles measured by QLS (D_p) at the end of the inverse microemulsion polymerization was 29.5 nm. After drying the particles and re-dispersing in water at 25 °C, the equilibrium water uptake of the polyNIPA nanoparticles was 12.9 $g_{water}/g_{xerogel}$.

The nanostructured hydrogels have strikingly different appearances and textures compared to the conventional polyNIPA hydrogels. The latter are firm and transparent (slightly hazy) in contrast to the nanostructured hydrogels that are opaque and become softer and more elastic as the content of particles increases.

Scanning electron microscopic photographs of the internal and external surfaces of the freeze-dried hydrogels at equilibrium swelling with $m_{particles}/m_{NIPA} =$ 30/70 and 0/100 are depicted in Figs. 1 and 2, respectively. Figure 1a shows the internal surface of the 30/70 sample, where irregularly shaped pores with sizes of 50–350 μm are observed. The corresponding external surface of the same sample (Fig. 1b) has a similar microstructure as that of the internal surface. Two features are also observed in this sample: low interconnection among pores and thicker pore walls. Figure 2a shows the internal surface of the 0/100 sample (i.e., the conventional hydrogel), which has a more homogeneous network of pores with thinner walls. An extensive interconnection among pores is observed. Pore size is in a narrow range of 70–150 μm. The microstructure corresponding to its external surface (Fig. 2b) is different to that of the internal surface, with smaller pores that have irregular shapes and sizes.

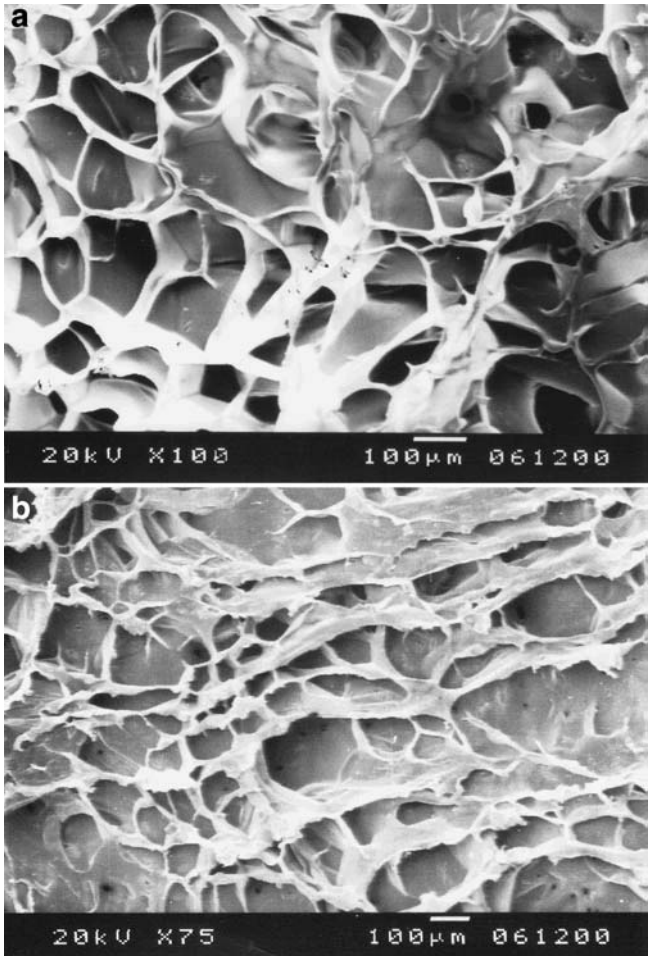

Fig. 1 Photographs taken by scanning electron microscope (SEM) of the internal (**a**) and external (**b**) surfaces of the nanostructured hydrogel made with $m_{particles}/m_{NIPA} = 30/70$

Differential scanning colorimetric thermograms of hydrogels at equilibrium water uptake with $m_{particles}/m_{NIPA}$ ratio of 0/100, 20/80 and 30/70 (not shown) reveal that the volume phase transition temperature was 33–34 °C for the conventional and the nanostructured hydrogels, regardless of $m_{particles}/m_{NIPA}$ ratio. This temperature is similar to that reported elsewhere [2].

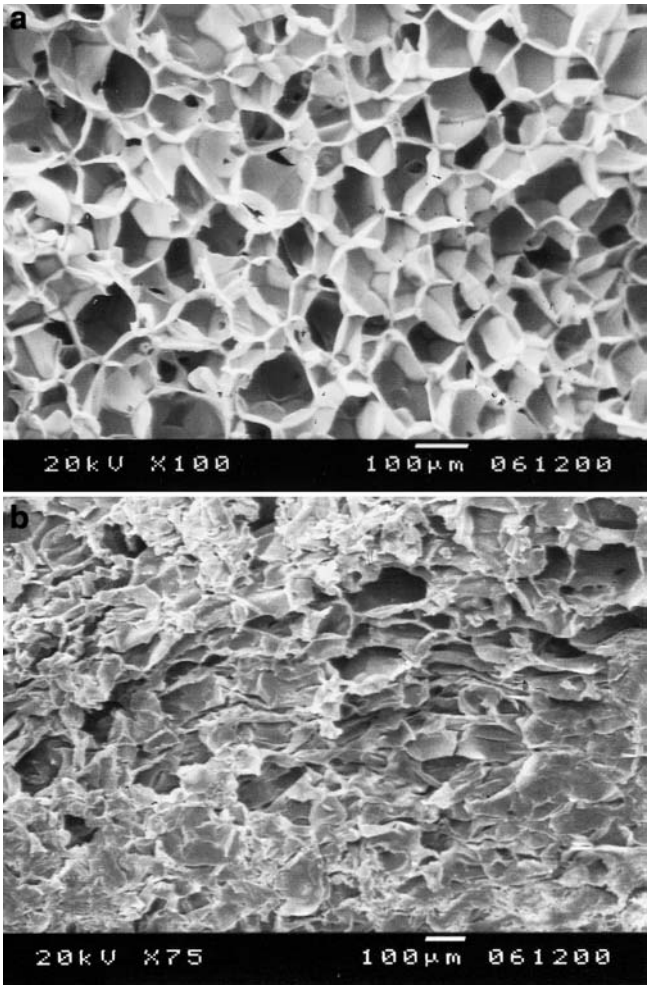

Fig. 2 Photographs taken by SEM of the internal (**a**) and external (**b**) surfaces of the conventional hydrogel

Figure 3 shows plots of H_p versus time for the hydrogels made with different $m_{particles}/m_{NIPA}$ ratios. For comparison, the swelling kinetics of a conventional hydrogel containing the same overall concentration of NIPA and made with the same concentrations of crosslinking agent and initiator is included in Fig. 3. The nanostructured hydrogels swell faster and have larger $H_{p\infty}$ values than the conventional hydrogel. Moreover, as the concentration of particles in the gel increases, the swelling rate (inset in Fig. 3) as well as the equilibrium water uptake increases.

Figure 4 depicts $H_{p\infty}$ as a function of temperature for the conventional and the nanostructured hydrogels made with different $m_{particles}/m_{NIPA}$ ratios. The equilibrium water uptake increases with increasing particle content for temperatures below the T_{VPT}, which was expected from the results depicted in Fig. 3. Moreover, for $T < T_{VPT}$, the slope of $H_{p\infty}$ versus temperature increases as the concentration of particles augments,

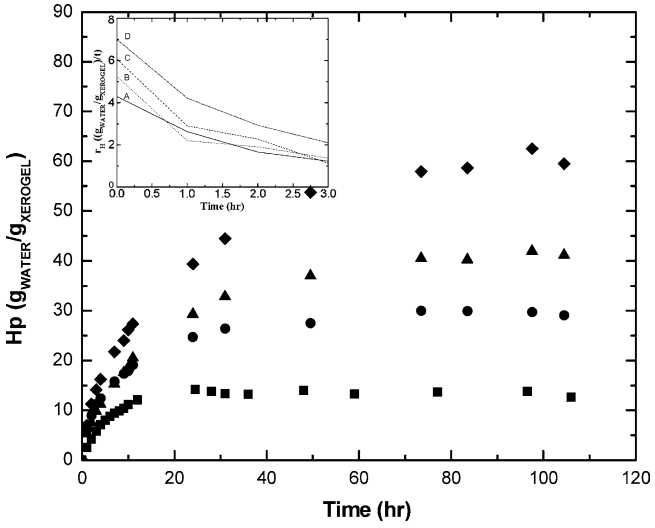

Fig. 3 Water uptake as a function of time for Poly(*N*-isopropylacrylamide) (polyNIPA) hydrogels prepared with varying weight ratios of NIPA to nanoparticles ($m_{particles}/m_{NIPA}$) in the second polymerization stage: (*filled square*) 0/100; (*filled circle*) 15/85; (*filled triangle*) 20/80; (*filled diamond*) 30/70. *Inset*: swelling rate as a function of time for polyNIPA hydrogels prepared with varying ($m_{particles}/m_{NIPA}$) ratios in the second polymerization stage: **a** 0/100; **b** 15/85; **c** 20/80; **d** 30/70

whereas at the T_{VPT} (ca. 35 °C), all the hydrogels collapse. Notice that the shrunk volume of the conventional gel is larger than those of the nanostructured materials. The solid lines represent the fitting obtained with Eq. 2. This equation was solved numerically with a constant χ_2 value of 0.41 and ν as the fitting parameter. The reported

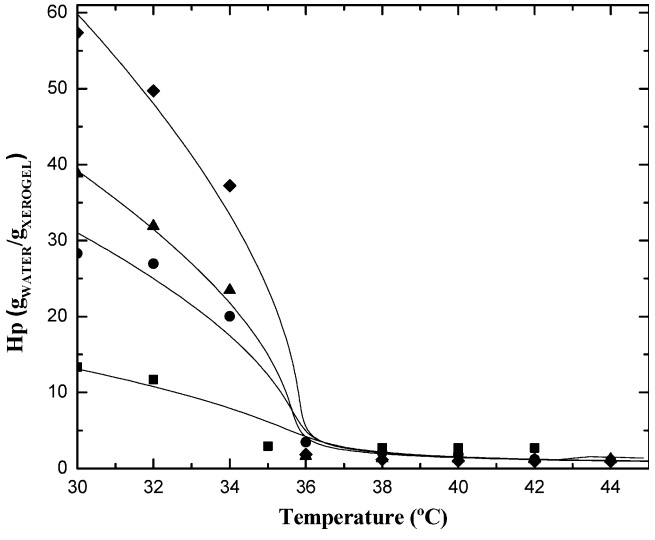

Fig. 4 Equilibrium water uptake as a function of temperature for polyNIPA hydrogels made with different $m_{particles}/m_{NIPA}$ in the second polymerization stage: (*filled square*) 0/100; (*filled circle*) 15/85; (*filled triangle*) 20/80; (*filled diamond*) 30/70. The *solids lines* represent the fitting of Eq. 2

value of χ_2 is 0.53, determined by applying the Flory–Rehner theory [53]. However, Takata et al. [54] found by small angle neutron scattering and the Panyukov–Rabin theory that the χ_2 of polyNIPA hydrogels in water depends on the temperature of preparation, obtaining values from 0.34 to 0.5 as the temperature reaches the collapsing temperature. Hence, within the experimental error, we believe the value used in our paper is reasonable. Table 1 shows the best-fitted ν-values.

Figure 5 depicts the de-swelling at 40 °C for hydrogels with $m_{\text{particles}}/m_{\text{NIPA}}$ of 0/100 and 15/85. Here, $F(t)$ $(= H_P\,(t)/H_{p\infty})$ represents the fraction of original water in the hydrogel at time t. Clearly, the nanostructured hydrogel de-swell much faster than the conventional one. Furthermore, the amount of water expelled from the nanostructured hydrogel is much larger inasmuch as the equilibrium swelling of the nanostructured gel doubles that of the conventional material.

The elastic and the Young moduli of the conventional and nanostructured hydrogels, obtained by TMA in the compression mode at $T < T_{\text{VPT}}$, are reported in Table 2. Both moduli decrease by the presence of the particles; however, the moduli are larger than those of conventional hydrogels with similar degree of equilibrium swelling (cf. Tables 2, 3). Notice that the E to G ratio is consistently larger than the ideal value ($E/G = 3$) obtained for ideal elastic networks [55].

Discussion and conclusions

PolyNIPA-based hydrogels are attractive materials that have important applications in medicine and bioengineering because of their thermoreversibility. For many of the applications of thermoreversible materials, the response rate to temperature variations is one of the most crucial functions and so, it is important to make this response faster. However, polyNIPA hydrogels are relatively hydrophobic, and so their equilibrium swellings are fairly low compared to more hydrophilic polymer gels, and their swelling and de-swelling rates are quite slow. Previously, we demonstrated that hydrogels with higher swelling and improved mechanical properties can be produced by incorporating polyacrylamide nanoparticles in a polyacrylamide matrix [27]. Moreover, we showed that the swelling kinetics becomes faster and the equilibrium water uptake higher as the concentration of nanoparticles in the polymer matrix was increased [27].

Here, we have demonstrated that similar effects are achieved by incorporating polyNIPA nanoparticles into a polyNIPA matrix. The rate of swelling is faster and the equilibrium swellings are two to four times higher than those of the conventional hydrogel prepared with similar overall concentrations of monomer ($m_{\text{NIPA}}/m_{\text{H}_2\text{O}} = 0.1$). and crosslinking agent ($m_{\text{NMBA}}/m_{\text{NIPA}} = 0.01$) (Fig. 4). Moreover, the rate of swelling and the maximum water uptake increase as the concentration of nanoparticles is increased (Fig. 4), similar to our previous findings [27]. The explanation to these results is that the polyNIPA nanoparticles have higher polymer concentration ($m_{\text{NIPA}}/m_{\text{H}_2\text{O}} = 0.25$). than the surrounding polyNIPA matrix ($m_{\text{NIPA}}/m_{\text{H}_2\text{O}} = 0.085$--$0.07$, depending on the weight ratio of nanoparticles to NIPA in the second stage of synthesis), even though the amount of crosslinking agent is similar in both stages ($m_{\text{NMBA}}/m_{\text{NIPA}} = 0.01$). SEM photographs clearly show that the nanostructured hydrogels have more open network structures (cf. Figs. 1, 2). Moreover, the particles swell with water, monomer and crosslinking-agent molecules before the second polymerization stage and so, when the NIPA (and NMBA) molecules within the particles polymerize and become incorporated to the crosslinked polymer chains forming in the aqueous solution, they give as a result a dendrite network (Fig. 6). In this stage, the particles are *trapped* into the polymer matrix because the new chains formed in the aqueous solution in the second stage are also crosslinked and entangled with the chains of the nanoparticles.

The resulting structure explains why the nanostructured materials have similar or larger modulus compared to the conventional hydrogels, even though their degree of swelling is much larger (cf. Tables 2, 3). Here we proposed that the anchorage polyNIPA particles act as reinforcement agents to improve the mechanical properties whereas the loose polyNIPA matrix allows larger swellings.

Table 1 Parameters used in the modified Flory–Rehner equation (Eq. 2) to predict data reported in Fig. 4

$m_{\text{part}}/m_{\text{NIPA}}$ (g/g)	Parameters								
	ν, Theoretic (mol/L)	ν, Exp (mol/L)	C_{NIPA}, (mM)	C_{NIPA0} (mM)	Φ_0	V_s, (L/mol)	$-\Delta H$, (J)	$-\Delta S$, (J/K)	χ_2
0	0.01297	0.01297	790	300	0.0799	0.018	12.46e-21	4.717e-23	0.41
15	0.0027	0.011	682	300	0.069	0.018	12.46e-21	4.717e-23	0.41
20	0.0018	0.0103	645	300	0.0653	0.018	12.46e-21	4.717e-23	0.41
30	0.00093	0.00908	570	300	0.0577	0.018	12.46e-21	4.717e-23	0.41

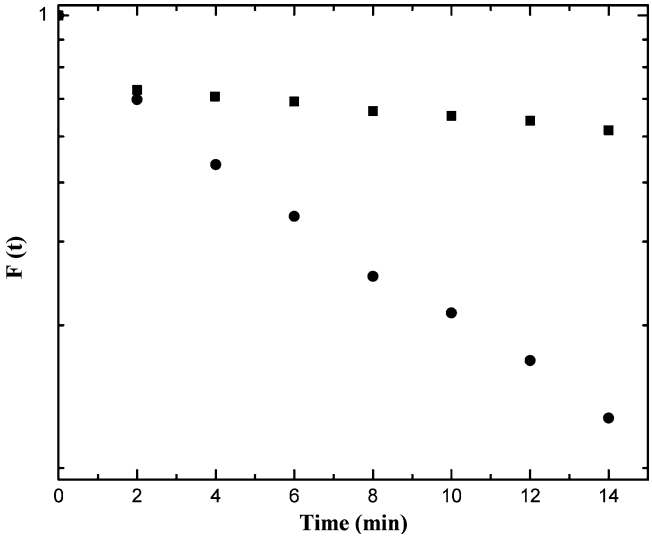

Fig. 5 De-swelling kinetics $F(t)$ as a function of temperature for polyNIPA hydrogels made with different $m_{particles}/m_{NIPA}$ in the second polymerization stage: (*filled square*) 0/100; (*filled circle*) 15/85

The ratio of E and G is larger than the value for ideal elastic material ($E/G = 3$) (Tables 2, 3, 4). Huglin et al. found similar results for copolymer hydrogels and provided the following explanation [49]. E is given by the slope of the linear region of Eq. 6 whereas G is the slope in the linear region of Eq. 7; hence by taking the derivative with respect to λ of Eqs. 6 and 7 and equating them, one obtains that $E = G(1 + 2\lambda^{-3})$. As expected, as $\lambda \rightarrow 1$, E/G should approach 3. However, in the compression tests performed here, λ is finite and negative, and so, E/G should be slightly larger than 3, in agreement with experimental results.

Since the conventional and the nanostructured hydrogels are made with the same polymer, it is not surprising that the volume phase transition temperature is the same in all the hydrogels (DSC results and Fig. 4). However, the amount of water expelled per weight of xerogel from the nanostructured hydrogels is substantially larger than that driven out from the conventional hydrogels and with faster expelling rate (Fig. 5). This can be important for controlled drug release applications.

Table 2 Young and elastic moduli of nanostructured hydrogels prepared at 25 °C as a function of the $m_{particles}/m_{NIPA}$ ratio and identical crosslinking degree (m_{NMBA}/m_{NIPA}) in the second polymerization stage

m_{part}/m_{NIPA} (g/g)	$H_{p\infty}$ ($g_{water}/g_{xerogel}$)	E (Pa)	G (Pa)	E/G
0/100	13.7	4725	1460	3.2
15/85	29.8	2760	850	3.2
30/70	58.9	2900	880	3.3

The swelling and de-swelling of a hydrogel are diffusion-limited processes and so, the rate is controlled by diffusion of water through the polymeric network. Hence, downsizing of the material is one way to increase the response rate. Also, it has been shown that the modification of the method of preparation can increase the rate of swelling and de-swelling [33–46]. Here we demonstrate that the incorporation of nanoparticles into the polymer matrix increases the rates of swelling (Fig. 3) and of de-swelling (Fig. 5). Moreover, the rate of water expulsion from the nanostructured hydrogels is similar to those reported from macroporous polyNIPA hydrogels [43] and from inhomogeneous polyNIPA hydrogels prepared at temperatures close to the T_{VPT} [46]. In fact, Takata et al. suggested that the rapid shrinking kinetics of the hydrogels made near the T_{VPT} is due to the formation of spatial inhomogeneities (polymer-poor and polymer-rich micro-domains) in the hydrogel network due to phase separation [46]. This explanation can be applied to our materials because the two-stage synthesis employed here introduces inhomogeneities (polymer-rich nanoparticles) into a polymer-poor matrix. However, in contrast to the method of Takata et al. [46], the inhomogeneities can be controlled in our method by varying the monomer and the crosslinking-agent concentrations during the first and second stages of the synthesis. In fact, the mechanical properties can also be modulated by the appropriated selection of NIPA and NMBA concentrations during the synthesis. Moreover, the same model proposed by Takata et al. for inhomogeneous polyNIPA gels with higher absorption capacities [46] was also used here rather successfully to reproduce the dependence of the equilibrium water uptake on temperature (Fig. 4).

To prove conclusively that the nanostructured hydrogels synthesized by us can be tailor-made for specific applications and have better swelling, de-swelling and mechanical properties compared to the temperature-induced inhomogeneous polyNIPA hydrogels [46] or to the macroporous polyNIPA hydrogels [43]; we made the macroporous and the temperature-induced inhomogeneous hydrogels following the recipes given in these papers. Similar to the reported values, these materials exhibited large equilibrium swelling as well as fast

Table 3 Equilibrium swelling, Young and elastic moduli of conventional hydrogels prepared at 25 °C as a function of NMBA/NIPA weight ratio

m_{NMBA}/m_{NIPA} (g/g)	$H_{p\infty}$ ($g_{water}/g_{xerogel}$)	E (Pa)	G (Pa)	E/G
0.001	24.4	2160	700	3.1
0.0025	23	3850	1270	3.0
0.005	18.5	4080	1310	3.1
0.0075	16.5	4440	1400	3.2
0.01	13.7	4720	14606	3.2

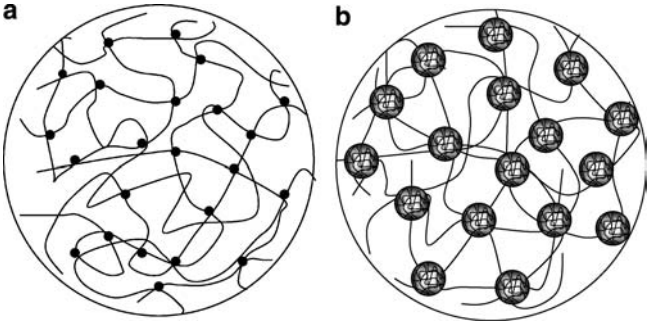

Fig. 6 Schematic description of the conventional (**a**) and microstructured (**b**) hydrogels

Table 4 Young and elastic moduli of temperature-induced inhomogeneous Poly(*N*-isopropylacrylamide) (polyNIPA) hydrogels made at different temperatures. The m_{NMBA}/m_{NIPA} ratio was equal to 0.01 in all cases

$T_{Preparation}$ (°C)	$H_p\infty$ ($g_{water}/g_{xerogel}$)	E (Pa)	G (Pa)	E/G
20	18.8	7150	2312	3.1
22	19.1	8600	2594	3.3
25	20.0	4719	1543	3.1
35	20.8	232	63	3.7

swelling and de-swelling kinetics, but they were quite fragile. In fact, it was possible to perform compression tests only on the temperature-induced inhomogeneous hydrogels but not on the macroporous hydrogels because they went to pieces during handling. We believe that the latter happened because the conversion of NIPA to polyNIPA dropped from 96.5% in the absence of PEG to ca. 50–60% when PEG was present in the reaction, and much faster swelling and de-swelling kinetics are expected in contrast to expecting very fragile materials as a result of the decrease of NIPA concentration, as reported elsewhere [43]. On the other hand, the equilibrium swelling of the temperature-induced inhomogeneous hydrogels increases with the temperature of preparation whereas the modulus decreases (Table 4). More importantly, the equilibrium swellings of our hydrogels are substantially larger than those of the temperature-induced inhomogeneous hydrogels, but their moduli are comparable probably because the amount and crosslinking degree of the inhomogeneities in the latter are not controlled (cf. Tables 2, 4).

In summary, a synthetic route involving inverse microemulsion polymerization followed by dispersion polymerization that permits the production of nanostructured hydrogels with faster swelling and de-swelling kinetics and improved mechanical properties was presented here. The novelty of the method is that it allows the introduction of a controlled number-density and size of polymer-rich domains into a polymer matrix. The swelling and de-swelling kinetics as well as the mechanical properties can be controlled by choosing the appropriate monomer and crosslinking-agent concentrations during the first and second stage, and by varying the weight ratio of particles to monomer in the second stage. More importantly, the monomers used in the first and second stages can be different and so, other properties such as the T_{VPT} (when one or both are thermoreversible) can be tailored. Reports on this type of hydrogels are underway (Fernández VVA, in preparation).

Acknowledgements We thank the support of CONACYT (grant# G-38725U). N. Tepale and VVA Fernández acknowledge CONACYT for the scholarships.

References

1. Taylor LD, Cerankowski LD (1975) J Polym Sci Polym Chem Ed 13:2551
2. Hirokawa Y, Tanaka T (1984) J Chem Phys 81:6379
3. Rinsdorff H, Simon J, Winnik FM (1992) Macromolecules 25:5353
4. Tanaka N, Matsukawa S, Kurosu H, Ando I (1998) Polymer 39:4703
5. Sun P, Li B, Wang Y, Ma J, Ding D, He B (2003) Eur Polym J 39:1045
6. Gutowska A, Bae YH, Jacobs H, Mohammad F, Mix D, Feijen J, Kim SW (1995) J Biomed Mater Res 29:811
7. Vakkalanka SK, Brazel CS, Peppas NA (1996) J Biomater Sci Polymer Ed 8:119
8. Ramkissoon-Ganorkar C, Liu F, Baudys M, Kim SW (1999) J Control Release 59:287
9. Chung JE, Yokoyama M, Yamato M, Aoyagi T, Sakurai Y, Okano T (1999) J Control Release 62:115
10. Chung JE, Yokoyama M, Okano T (2000) J Control Release 65:93
11. Zhang J, Pepas NA (2000) Macromolecules 33:102
12. Kikuchi A, Okano T (2002) Adv Drug Deliver Rev 54:53
13. Hoffman AS (2002) Adv Drug Deliver Rev 54:3
14. Kumar MNVR, Kumar N, Domb AJ, Arora M (2002) Adv Polym Sci 160:54
15. Osada Y, Okuzaki H, Hori H (1992) Nature 355:242
16. Shiino D, Murata Y, Kataoka K, Koyama Y, Yokoyama M, Okano T, Sakurai Y (1994) Biomaterials 15:121
17. Freitas RFS, Cussler EL (1987) Chem Eng Sci 42:97
18. Champ S, Xue W, Huglin MB (2001) Polymer 42:6439
19. Stayton PS, Shimobji T, Long C, Chilkoti A, Chen G, Harris JM, Hoffman AS (1995) Nature 378:472
20. Chu L-Y, Park S-H, Yamaguchi T, Nakao S (2001) J Membr Sci 192:27
21. Dong LC, Hoffman AS (1986) J Control Release 4:223
22. Stile RA, Burghardt WR, Healy KE (1999) Macromolecules 32:7370

23. Johnson BD, Beebe DJ, Crone WC (2004) Mat Sci Eng C 24:575
24. Zhang X-Z, Wu D-Q, Chu C-C (2004) Biomaterials 25:3793
25. Liu RH, Yu Q, Beebe DJ (2002) J Microelectromech Syst 11:45
26. Mournir A, Darwish N, Shehata A (2004) J Appl Polym Sci 91:3921
27. Puig LJ, Sánchez-Díaz C, Villacampa M, Mendizábal E, Puig JE, Aguiar A, Katime I, (2001) J Colloid Interface Sci 235:278
28. Kudela V (1987) Hydrogels. In: Mark HF, Bikales NM, Overberger CG, Menges G (eds) Encyclopedia of polymer science and engineering. Wiley, New York, pp 783–807
29. Yasuda H, Refofo MF (1964) J Polym Sci A-2:5093
30. Mathur AM, Moorjani SK, Scranton AB (1996) Rev Macromol Chem Phys C 36(2):405
31. Funke W, Okay O, Joos-Müller B (1998) Microgels—intramolecularly crosslinked macromolecules with a globular structure. Adv Polym Sci 136:139–234
32. Pelton R (2000) Adv Colloid Interf Sci 85:1
33. Kabra BG, Gehrke SH (1991) Polym Commun 32:322
34. Wu XS, Hoffman AS, Yager P (1992) J Polym Sci Polym Chem Ed 30:2121
35. Yoshida R, Uchida K, Kaneko Y, Sakai K, Kikuchi A, Sakurai Y, Okano T (1995) Nature 374:240
36. Kaneko Y, Sakai K, Kikuchi A, Yoshida R, Sakurai Y, Okano T (1995) Macromolecules 28:7717
37. Kaneko Y, Nakamura S, Sakai K, Aoyaji T, Kikuchi A, Sakurai Y, Okano T. (1998) Macromolecules 31:6099
38. Zhang X-Z, Zhuo RX (1999) Colloid Polym Sci 277:1079
39. Zhang X-Z, Zhuo RX (1999) Macromol Chem Phys 200:2602
40. Zhang X-Z, Zhuo RX (2000) J Colloid Interface Sci 223:311
41. Zhang X-Z, Zhuo RX (2001) Langmuir 17:12
42. Zhang X-Z, Zhuo RX (1999) Macromol Rapid Commun 20:229
43. Zhang X-Z, Yang Y-Y, Chung T-S, Ma K-X (2001) Langmuir 17: 6094
44. Shibayama M, Shirotani Y, Hirose H, Nomura S (1997) Macromolecules 30:7307
45. Shibayama M, Nagai K (1999) Macromolecules 32:7461
46. Takata S, Suzuki K, Norisuye T, Shibayama M (2002) Polymer 43:3101
47. Ofner CM III, Schott H (1986) J Pharm Sci 75:790
48. Ofner CM III, Schott H (1987) J Pharm Sci 76:715
49. Keys KB, Andreopolous FM, Peppas NA (1998) Macromolecules 31:8149
50. Vamvakaki M, Hadjiyannakou SC, Loizidou E, Patrickios CS, Armes SP, Billingham NC (2001) 13:4738
51. Lutz PJ (2001) Macromol Symp 164:277
52. Huglin MB, Rehab MMA-M, Zakaria MB (1986) Macromolecules 19:2986
53. Erbil C, Aras S, Uyanik N (1999) J Polym Sci Part A Polym Chem 37:1847
54. Takata S, Norisuye T, Shibayama T (2002) Macromolecules 35:4779
55. Ferry JD (1980) Viscoelastic properties of polymers. Wiley, New York